

# Changes in hip Joint Contact Stress During a Gait Cycle based on the Individualized Modeling Framework of "Gait-Musculoskeletal System-Finite Element"

**Binglang Xiong**

Guangzhou University of Chinese Medicine

**Peng Yang**

Guangzhou University of Chinese Medicine

**Tianye Lin**

Guangzhou University of Chinese Medicine

**Jinli Xu**

Guangzhou University of Chinese Medicine

**Yong Xie**

Guangzhou University

**Yongliang Guo**

Jinan University

**Churong Liu**

Jinan University

**Qizhao Zhou**

Guangzhou University of Traditional Chinese Medicine: Guangzhou University of Chinese Medicine

**Qizhong Lai**

Guangzhou University of Chinese Medicine

**Qiushi Wei**

Guangzhou University of Chinese Medicine

**Wei He**

Guangzhou University of Chinese Medicine

**Qingwen Zhang** (✉ [zhangqingwen1121@163.com](mailto:zhangqingwen1121@163.com))

Guangzhou University of Chinese Medicine <https://orcid.org/0000-0002-5685-7420>

---

## Research Article

**Keywords:** Gait, musculoskeletal system, finite element analysis, hip biomechanics

**Posted Date:** October 28th, 2021

**DOI:** <https://doi.org/10.21203/rs.3.rs-983381/v1>

**License:**  This work is licensed under a Creative Commons Attribution 4.0 International License. [Read Full License](#)

# Abstract

**Objective:** To construct a comprehensive simulation framework of "gait-musculoskeletal system(MS)-finite element(FE)" for analysis of hip joint dynamics characteristics and the changes in the contact stress in the hip throughout a gait cycle.

**Methods:**Two healthy volunteers (male and female) were recruited. The 3D gait trajectories during normal walking and the CT images including the hip and femur of the volunteers were obtained. CT Imaging data in the DICOM were extracted for subjected 3D hip joint reconstruction. The reconstructed 3D model files were used to realize the subject-specific registration of the pelvis and thigh segment of general musculoskeletal model. The captured marker trajectory data were used to drive subject-specific musculoskeletal model to complete inverse dynamic analysis. Results of inverse dynamic analysis were exported and applied as boundary and load settings of the hip joint finite element in ABAQUS. Finally, the finite element analysis(FEA) was performed to analyze contact stress of hip joint during a gait cycle of left foot.

**Results:** In the inverse dynamic analysis, the dynamic changes of the main hip-femoral muscle force with respect to each phase of a single gait cycle were plotted. The hip joint reaction force reached a maximum value of 2.9%BW (Body weight) and appeared at the end of the terminal stance phase. Twin peaks appeared at the initial contact phase and the end of the terminal stance phase respectively. FEA showed the temporal changes in contact stress in the acetabulum. In the visual stress cloud chart, the acetabular contact stress was mainly distributed in the dome of the acetabulum and in the anterolateral area at the top of the femoral head during a single gait cycle. The acetabular contact area was 293.8-998.4 mm<sup>2</sup> and the maximum contact area appear at the mid-stance phase or the loading response phase of gait. The maximum contact stress of the acetabulum reached 6.91 Mpa (Model 1) / 6.92 Mpa (Model 2) at the terminal stance phase.

**Conclusions:**The "Gait-MS-FE" technology is integrated to construct a comprehensive simulation framework. Based on human gait trajectories and their CT images, individualized simulation modeling can be achieved. Subject-specific gait in combination with an inverse dynamic analysis of the MS provides pre-processing parameters for FE simulation for more accurate biomechanical analysis of hip joint.

## Introduction

Hip arthritis as one of the most common hip diseases is projected to affect 411,000 people in the United States by 2030[1]. Without appropriate treatment for a long time, it will affect daily walking due to chronic pain in the knee and the spine and other symptoms[2, 3], and eventually, through 2030, 572,000 patients will undergo the cost-consuming hip replacement surgery per year [4, 5]. Therefore, studies about hip joint biomechanics to better understand the occurrence and development of hip diseases have significant clinical and economic implications. Hip joint as the largest joint in the human body features intricate biomechanics. To achieve more accurate hip biomechanics, it is a high priority to consider an integrated forces from skeletal structures, as well as surrounding muscles and ligaments of hip joint motion[6]. Moreover, in reality, the hip joint is always in constant motion to complete different activities. In a complete gait cycle, different mechanical states of the hip joint [8] remind us that gait characteristics should also be taken into account for biomechanics studies about the hip joint. However, most of the previous research literature on the FE mechanics of the hip joint adopted a simplified model of one-foot standing, only considering the mechanical state of the hip when standing, and believed that the hip bears the

greatest force at this time[9–11],We conducted this research with skepticism and established the "Gait-MS-FE" hip joint mechanics research framework to explore the changes in hip joint contact stress during a gait cycle.

In recent years, the MS based on muscle forces has become an indispensable technique that underpinned optimal designs of treatment strategies and medical products[12]as it can better simulate the shapes of various parts of the most intricate joint. However, it also meets a bottleneck of individualized simulation.In previous biomechanical studies, the muscle forces around one person's joints obtained in the laboratory were loaded into another person's FE model in the form of loads, while ignoring the differences in individualized muscle forces and the difference in hip joint morphology.these did not achieve individualized research.Some studies using the FEA have concluded that different pathological morphologies of the hip joint can affect the body-weight loading onto the articular cartilage [13–18].The shape of the hip joint of normal people are also slightly different.A study by Anderson et al. [19] reported that differences in hip morphology among individuals have a great effect on the contact stress distribution in the hip joint.And there are differences in gait between individuals.The finite element model, the loaded muscle force and gait data used in our study are all from the same volunteer, which can truly achieve a personalized study of hip joint Biomechanics, eliminating the interference of other individual differences.

In this study, the human hip joint was individually simulated using the "gait-MS-FE" framework to reconstruct a dynamic hip joint model more accurately.Our purpose is to analyze the changes in the contact stress of the hip joint during a gait cycle, and the conclusions obtained can be used to optimize clinical decision-making and lay the foundation for future hip joint biomechanical research,The method used in this study can be used for other personalized research on joint biomechanics.

## Methods

### Data collection

A healthy male volunteer (32 years of age, 70 kg, 171 cm) and a healthy female volunteer (27 years of age, 51 kg, 162 cm) were included in our study. The following gait kinematic data of the two volunteers during the current experiment and the follow-up period were obtained.

### Imaging data:

Candidates who had abnormalities in pelvic posture and hip morphology in pelvic X-ray and CT imaging were excluded. The region from 1 cm above the highest point of the iliac crest to 3 cm below the trochanter was scanned using X-ray. The pelvis and the femur were examined by CT (0.5 mm slice thickness, 5 mm wavelength interval, and image resolution of 1024×1024). CT images were saved as DICOM format and exported for 3D rigid-body modeling.

### Gait kinematic data:

Hip position data of standing posture and gait data of volunteers during walking were collected using the optical 3D gait analysis system (BTS Bioengineering, Italy). During the experiment, the two participants received adaptive training to walk continuously and freely prior to the tests. Then, they underwent 3 rounds of 5-m walk tests to ensure that both feet stepped into the force platform during at least one complete gait cycle in the one-way

walking path. Infrared reflective markers were attached to the trunk, arms and legs and gait trajectories were formally collected and saved as the C3D file format for subsequent procedures.

## **Subject-specific musculoskeletal dynamics simulation**

The dynamic hip motion of musculoskeletal model was simulated in the AnyBody modeling system (AnyBody Technology Company, Denmark). Custom musculoskeletal dynamics and inverse dynamics were analyzed using a modified fullbody model. As the function and application of AnyBody were reported elsewhere[20]; this article focused on the custom simulation process.

### **Model customization:**

To preliminarily adjust scaling, the body fat was measured using the built-in formulas in the AnyBody modeling system (volunteers' BMI: 23.94/ 19.4). To achieve a more accurate self-customization, DICOM data extracted from CT images were used for 3D reconstruction of the ilium and femur using Mimics software (version 16.0, Materialise, Belgium) (Figure 1). After reconstruction, 3D model files were imported into AnyBody for morphological scaling to realize the subject-specific registration of the pelvis and thigh segment of general musculoskeletal model in AnyBody based on spatial coordinates of the characteristic points of the iliofemoral models by point-to-point scaling codes. Moreover, the scaling was adjusted to match the starting and ending points of the muscles and ligaments surrounding the hip joint so that the anatomical features of human hip movements could be simulated more accurately.

### **Gait customization:**

C3D files containing volunteers' gait data were imported to AnyBody, and the locations of virtual markers alongside their 3D coordinates were adjusted to create the fully-matched models in accordance with the locations of markers attached to the trunk, arms and legs of volunteers. The simulated models were optimized using the built-in kinematic-parameter optimization algorithm in AnyBody which called kinematics optimization, and simultaneously the movement angles of the hip, knee, and ankle joints and the excursion of markers were calculated. The dynamic hip motion containing 8 phases in a gait cycle was simulated using the each one of optimized multibody model (Fig.2).

## **Inverse dynamic analysis**

Data obtained through kinematics optimization above were re-extracted for inverse dynamics analysis. Muscle recruitment was solved by formulating a third-order polynomial optimization problem. After the musculoskeletal models completed corresponding walking gait during inverse dynamics loading, the data of muscle forces and joint reaction forces of the legs were obtained (Fig.3). Data of the muscle strength and the kinematics of the hip during a complete gait cycle were extracted for verification.

# FEA for the contact stress distribution in the left hemipelvis FE models

## Geometric definition:

While subject-specific geometric cartilage model is crucial for biomechanical analysis. Bone morphology has been reported to play an important role to predict cartilage stress[21], it has also been shown that the optimal alignment of the joint was not sensitive to the choosing of cartilage thickness distribution. Therefore, we performed an 3D dilation on the surface of the femoral head and lunate surface of acetabular fossa to reconstruct a constant thickness (1.8 mm) cartilage layers of the femur and acetabulum[21].

## Material properties and boundary conditions:

As illustrated elsewhere[22], the cartilage of a normal hip joint was modeled using homogeneous, isotropic and linear elastic materials, while the cortical bone and trabecular of the ilium and femur were modeled using homogeneous isotropic materials (Table 1).

According to the method described elsewhere[23], data of the 8 phases during a single gait cycle of the left foot were introduced to analyze the contact stress of the hip joint during walking using the FEA. In the FE model, rigid transformation parameters of the hip during a gait cycle were adjusted using the kinematic data from the musculoskeletal simulation analysis, and realized by rotating coordinates of all unit nodes of the femur part. Assuming that the original coordinate of the femoral node was  $P(x_0, y_0, z_0)$ , the angles of hip rotation along the three axes of  $x$ ,  $y$ , and  $z$  were  $\theta_x$ ,  $\theta_y$ , and  $\theta_z$ , and then the three rotation matrices were:

$$A = \begin{bmatrix} 1 & 0 & 0 \\ 0 & \cos \theta & -\sin \theta_x \\ 0 & \sin \theta & \cos \theta_x \end{bmatrix} \quad (1-1)$$

$$B = \begin{bmatrix} \cos \theta_y & 0 & -\sin \theta_y \\ 0 & 1 & 0 \\ \sin \theta_y & 0 & \cos \theta_y \end{bmatrix} \quad (1-2)$$

$$C = \begin{bmatrix} \cos \theta_x & \sin \theta_x & 0 \\ -\sin \theta_x & \cos \theta_x & 0 \\ 0 & 0 & 1 \end{bmatrix} \quad (1-3)$$

Based on a standard boundary condition described by Phillips et al.[24], data constraints were applied to the top of the ilium and pubic areas when all 6 degrees of freedom were constrained to 0. The rotation center of the femoral head obtained by a least-squares spherical fitting was selected as the reference node, and the nodes on the femoral head surface were constrained by the reference node using a kinematic coupling. The resultant force was applied at the reference point, and the direction of the resultant force at each gait phase were consistent with the reaction force (including the corresponding muscle forces[20] of the hip joint derived from inverse dynamics

analysis). The interaction between the femoral head and the acetabulum was simulated by face to face contact in ABAQUS, and the contact was assumed to be frictionless as it was used elsewhere[25].

The mesh sensitivity was performed on a cartilage component rather than the skeletal for contact stress analysis, since we mainly focus on the contact stress of the hip joint, and a finer mesh was used. Three different mesh sizes were tested on the cartilage models, and the suitability was assessed based on the results of the contact stress analysis (the mesh selection criteria was defined as the changes in contact pressure and area with the difference between the meshes within 1%).

Table 1

Properties of materials, the number of elements and elastic modulus in FE models

Components	Element type	Number of elements	Elastic modulus (MPa)	Poisson's ratio
Cortical bone (femur + ilium)	C3D10	Model 1: 22827	15100	0.3
		Model 2: 19881		
Trabecular bone (femur + ilium)	C3D10	Model 1: 45642	445	0.22
		Model 2: 41043		
Cartilage (femoral head)	C3D10M	Model 1: 56783	15	0.45
		Model 2: 51480		
Cartilage (acetabulum)	C3D10M	Model 1: 60100	15	0.45
		Model 2: 56104		

## Results

### Muscle force patterns

After kinematics optimization, the AnyBody musculoskeletal models successfully completed gait trials containing complete gait cycles. Data of a single gait cycle (men: 1.17s, women: 1.31s) of the left foot was used for the inverse dynamic analysis. The simulated muscle force patterns in each gait phase during a normal gait cycle were basically consistent with the predicted results described elsewhere [26]. The gluteus maximus, gluteus medius, biceps femoris, quadriceps femoris and adductor magnus showed peak muscle forces at the initial contact phase, while the short external rotator muscles consisting of the **gluteus minimus**, iliopsoas, and adductor longus showed peak muscle forces at the end of the terminal stance phase (Fig.4). The hip joint reaction force reached a maximum value of 2.9%BM at the end of the terminal stance phase. Twin peaks appeared at the initial contact phase and the end of the terminal stance phase respectively (Fig.5).

### Contact mechanics of the hip joint

The contact stress distribution of the hip joint during each phase of a normal gait cycle was analyzed by FEA, and results showed that the contact stress at each phase were consistent with the reaction forces of the hip joint. The FEA results showed the time-phase change characteristics of the contact stress distribution of the acetabulum. A double peak of the peak contact pressure was detected at the loading response phase and the end of the terminal stance phase, during which the maximum contact stress reached 6.91 mpa in Model 1 and 6.92 mpa in Model 2 (Table 2). This results was in conformity with the previous findings[27]. During a complete gait cycle, the contact pressure was mainly distributed at the top of the femoral head and the dome of the acetabulum, and moved from the anterior column to the posterior column of the acetabulum from phase 1 to phase 8 (Fig.6). The contact areas were 316.7-787.6 mm<sup>2</sup> in Model 1 and 293.8-998.4 mm<sup>2</sup> in Model 2. Model 1 reached a maximum of 787.6mm<sup>2</sup> at the mid-stance phase while Model 2 reached a peak of 998.4 mm<sup>2</sup> at the loading response phase.

Table. 2

Hip joint reaction forces, peak contact pressure and contact area changes during different phases of a gait cycle\*

Phases of a gait cycle	Components ( $F_x, F_y, F_z$ ) of hip joint reaction forces (N)						Peak contact pressure (MPa)		Contact area (mm <sup>2</sup> )	
	Model 1			Model 2			Model 1	Model 2	Model 1	Model 2
	$-F_x$	$-F_y$	$-F_z$	$-F_x$	$-F_y$	$-F_z$				
1	89.32	746.57	171.35	29.23	737.69	182.3	3.87	3.78	607.2	548.3
2	517.5	1706.6	636.6	241.27	1472.22	300.8	6.72	5.88	720.4	998.4
3	151.03	1211.7	404.1	103.97	1053.17	222.22	6	5.78	787.6	717.4
4	-6	1562.5	442.43	67	1372.2	377.38	6.91	6.92	758.1	943.2
5	-34.15	1837.55	342.37	11.67	1622.1	178.21	6.72	6.1	721.1	912.2
6	172.64	932.92	237.38	231.22	1033.38	334.17	2.88	3.5	589.3	672.2
7	91.23	478.7	243.72	45.22	344.83	177.31	2.06	1.52	316.7	238.8
8	92.67	717.3	172.74	37.18	710.26	177.9	3.24	3.32	586.4	426.1

\*Force components ( $F_x, F_y, F_z$ ) corresponded to the local coordinate system of the thigh in MS models. Peak contact pressure and contact area were detected using the FE analysis.

## Discussion

In this study, volunteers' gait data was collected, and then a musculoskeletal model was created and reverse dynamic analysis was performed. We use the results of the inverse dynamic analysis as the boundary and load settings of the finite element model of the hip joint, then FEA was used to analyze the contact stress of the hip joint at each phase in a complete gait cycle. This study confirmed that the hip joint reaction was constantly changing during a complete gait cycle, and the contact stress was the highest at the terminal stance phase. There were double peaks at the the loading response phase and the end of the terminal stance phase, but not in themid-stance phase.

However, most of previous studies about contact mechanics of legs using the FE model were based on a standing position [28–31], which could simplify the analysis and could not objectively reflect dynamic stress distribution. So it was easy to underestimate the damages of the contact stress, and the relevant researches results could not truly reflect the human body. Based on the results of our research, we believe that if an in-depth study of hip joint mechanics is carried out, a lot of important details may be overlooked by simply using the standing model. Our research results may also indirectly optimize clinical decision-making and improve the design of joint-related products. Studies have shown that excessive stress on the hip joint was the main cause of hip arthritis [32, 33], which also reminds us that patients with clinical hip arthritis are more prone to joint aging in these two periods. Another findings of our study were that the acetabular contact stress was mainly distributed in the medial part of the dome of the acetabulum and the anterolateral part of the top of the femoral head, moving from the anterior column to the posterior column of the acetabulum during a gait cycle. Therefore, in the daily diagnosis and treatment of femoral head necrosis, we must focus on the anterolateral part of the top of the femoral head to predict a collapse early on as this area bears the most concentrated forces at the early stage. This result is also helpful for guiding the daily rehabilitation exercise of patients with femoral head necrosis and for providing valuable recommendations for the selection of treatment regimens.

Few studies have analyzed changes in the dynamic contact stress distribution during a gait cycle. Brown et al. [34] implanted a resistive sensor on the surface of the acetabular cartilage in vivo to monitor the surface mechanics. The results obtained by this method, though relatively reliable, are highly invasive, technically demanding and cost-consuming. Guangye Wang et al [35] analyzed the stress distribution during a normal gait cycle using the FEA, and concluded that in a complete gait acetabulum contact stress presented bimodal distribution and the peak appeared in the starting phase and the support phase, respectively, with the maximum stress ranging from 4.2 to 3.3 MPa. Moreover, the acetabulum contact area reached the maximum, of 1470 mm<sup>2</sup>, in the initial phase. Anderson et al [36] showed that the maximum contact stress of the acetabulum during a walking gait was 10.78 mpa. After the FE analysis for 10 healthy volunteers, Michael d. hyarris et al [37] believed that the acetabular contact stress reached its peak (7.52±2.11 mpa) when walking on the heel, and the average contact area occupied 34% of the total acetabular area. A study by Wu et al [38] reported that in a gait cycle the maximum contact pressure reached 7.48 MPa. Their results are inconsistent with other studies and it can be explained by their failure to consider impacts from the surrounding soft tissues such as muscles and ligaments. Besides, there are still differences between simulated data and gait trajectories of subjects. Li 's [39] study uses the same as this study to use the MS and FEA for coupling modeling. The results found that the maximum contact stress of the hip joint is 6.5Mpa presented to the initial contact phase, which is close to the results of this study. However, the gait data it used was taken from public databases, not from the same researcher, and it failed to achieve personalized research. Our research uses the "Gait-MS-FE" framework to add muscle strength around the joints to the model, which also reduces the influence of gait differences between individuals on the results of the study, so the results of this study are more credible.

The innovation of our research is that the framework of "gait-MS-FE" is applied to the study of hip joint mechanics, and to personally study the changes in the contact stress of the hip joint during a gait cycle. This framework can also be applied to the research of the contact stress changes of the hip in special positions and the contact stress of certain hip diseases. Genda, et al [40] analyzed and compared the contact stress between 112 healthy individuals and 66 patients, and the results showed that the contact stress in the normal acetabulum can be evenly distributed on the surface of the joints, and the articular contact stress in patients with joint dysplasia relatively concentrated on the anterior lateral edges of the acetabulum. However, the study only studied the contact stress in a stationary

state and failed to pay attention to the characteristics of the entire gait. Robert et al. [41] studied the changes of the acetabular contact stress in 12 patients who had undergone periacetabular rotational osteotomy for nearly 10 years, which had a clinical implication for the treatment of hip dysplasia. However, the dynamic analysis of the whole gait process was lacking and the effect of the surrounding muscle force on the results was not considered. If the "gait-MS-FE" framework is applied to the research of these diseases, it may make the research results more realistic.

However, limitations in this study must be acknowledged. Like most studies about the FEA [42–45], all bone models are treated with homogenization, while the actual bone density of different parts is uneven. In this regard, some errors may exist in our study. In addition, this study failed to consider the influence of different walking speeds on the contact stress of the hip joint, Hu et al [46] found that changes in walking speed may lead to changes in joint mechanics. In addition, this study failed to consider the muscle forces on other joints such as the knee joint, which may also have an impact on the contact stress of the hip joint.

To sum up, Subject-specific gait in combination with an inverse dynamic analysis of the MS provides pre-processing parameters for finite element simulation for more accurate biomechanical analysis of hip joint. In this study, the contact stress of the hip joint in a gait cycle was studied by constructing the "gait-MS-FE" framework, and the conclusions reached were more accurate. The method used can also be used for the mechanical research of other joints.

## Abbreviations

MS: musculoskeletal system; FE: finite element; BW: body weight; FEA: finite element analysis

## Declarations

## Acknowledgements

Not applicable

## Authors' Contributions

X.B.L. was responsible for the design and implementation of the study presented. Y.P. and L.T.Y. were responsible for the development of the finite-element models. L.T.Y. and X.J.L. conducted the experiments and were responsible for the acquisition of the data. Z.Q.Z. and L.Q.Z. were responsible for recruiting volunteers. G.Y.L. and L.C.R. provided technical support for gait analysis (BTS Bioengineering, Italy). X.B.L. prepared the initial draft of the manuscript. Z.Q.W., W.Q.S. and H.W. gave critical feedback during the study and critically revised the submitted manuscript for important intellectual content. All authors have read and approved the final manuscript to be submitted.

## Funding

The authors acknowledge the Natural Science Foundation of China (Grant No. 81873327), Natural Science Foundation of Guangdong (Grant No. 2015A030313353), Scientific Research Project of Chinese Medicine of

Guangdong (Grant No. 20191116) and Excellent Doctoral Dissertation Incubation Grant of First Clinical School of Guangzhou University of Chinese Medicine (Grant No. YB201802).

## Availability of data and materials

Not applicable

## Ethics approval and consent to participate

All procedures of this study were in accordance with the ethical standards laid down in the 2013 Declaration of Helsinki and approved by the Ethics Committee of the First Affiliated Hospital of Guangzhou University of Chinese Medicine (No. K [2019]124).

## Consent for publication

Not applicable

## Competing interests

The authors declare no competing interests.

## References

1. Quinn RH, Murray J, Pezold R, Hall. Q(2018)Management of Osteoarthritis of the Hip. *J Am Acad Orthop Surg*,26(20):e434-e436.
2. Stief F, Schmidt A, van Drongelen S, Lenarz K, Froemel D, Tarhan T, Lutz F,Meurer A(2018). Abnormal loading of the hip and knee joints in unilateral hip osteoarthritis persists two years after total hip replacement [published online ahead of print. *J Orthop Res*,2018;10.1002/jor.23886.
3. Warashina H, Kato M, Kitamura S, Kusano T, Hasegawa Y. The progression of osteoarthritis of the hip increases degenerative lumbar spondylolisthesis and causes the change of spinopelvic. alignment *J Orthop*. 2019;16(4):275–9.
4. Nho SJ, Kymes SM, Callaghan JJ, Felson. DT(2013)The burden of hip osteoarthritis in the United States: epidemiologic and economic considerations. *J Am Acad Orthop Surg*,21Suppl 1:S1-S6.
5. Koenig L, Zhang Q, Austin MS, Demiralp B, Fehring TK, Feng C, Mather RC,Nguyen JT,Saavoss A,Springer BD, Jr *AJY*(2016). Estimating the Societal Benefits of THA After Accounting for Work Status and Productivity: A Markov Model Approach. *Clin Orthop Relat Res*,474(12):2645-2654.
6. Polkowski GG, Clohisy. JC(2010)Hip biomechanics. *Sports Med Arthrosc Rev*,18(2):56–62.
7. Zhang C, Li L, Forster BB, Kopec AJ, Ratzlaff C, Halai L, Cibere J, Esdaile JM. Femoroacetabular impingement and osteoarthritis of the hip. *Can Fam Physician*. 2015;61(12):1055–60.
8. Wootten ME, Kadaba MP, Cochran. GV(1990)Dynamic electromyography. II. Normal patterns during gait. *J Orthop Res*,8(2):259–265.

9. Vogel D, Wehmeyer M, Kebbach M, Heyer H, Bader R. Stress and strain distribution in femoral heads for hip resurfacing arthroplasty with different materials: A finite element analysis. *J Mech Behav Biomed Mater.* 2021;113:104115.
10. Xu J, Zhan S, Ling M, Jiang D, Hu H, Sheng J, Zhang C. Biomechanical analysis of fibular graft techniques for nontraumatic osteonecrosis of the femoral head: a finite element analysis. *J Orthop Surg Res.* 2020;17(1):335–15(.
11. Akrami M, Craig K, Dibaj M, Javadi AA, Benattayallah A. A three-dimensional finite element analysis of the human hip. *J Med Eng Technol.* 2018;42(7):546–52.
12. Jonkers I, Sauwen N, Lenaerts G, Mulier M, Van der Perre G, Jaecques S. Relation between subject-specific hip joint loading, stress distribution in the proximal femur and bone mineral density changes after total hip replacement. *J Biomech.* 2008;41(16):3405–13.
13. Yoshida H, Faust A, Wilckens J, Kitagawa M, Fetto J. Chao EY(2006)Three-dimensional dynamic hip contact area and pressure distribution during activities of daily living. *J Biomech*,39(11):1996–2004.
14. Russell ME, Shivanna KH, Grosland NM, Pedersen. DR(2006)Cartilage contact pressure elevations in dysplastic hips: a chronic overload model. *J Orthop Surg Res*,1:6.
15. Chegini S, Beck M, Ferguson. SJ(2009)The effects of impingement and dysplasia on stress distributions in the hip joint during sitting and walking: a finite element analysis. *J Orthop Res*,27(2):195–201.
16. Henak CR, Abraham CL, Anderson AE, Maas SA, Ellis BJ, Peters CL. Weiss JA(2014)Patient-specific analysis of cartilage and labrum mechanics in human hips with acetabular dysplasia. *Osteoarthritis Cartilage*,22(2):210–217.
17. Hellwig FL, Tong J, Hussell. JG(2016)Hip joint degeneration due to cam impingement: a finite element analysis. *Comput Methods Biomech Biomed Engin*,19(1):41–48.
18. Ng KC, Mantovani G, Lamontagne M, Labrosse MR, Beaulé. PE(2017)Increased Hip Stresses Resulting From a Cam Deformity and Decreased Femoral Neck-Shaft Angle During Level Walking. *Clin Orthop Relat Res*,475(4):998–1008.
19. Anderson AE, Ellis BJ, Maas SA, Weiss. JA(2010)Effects of idealized joint geometry on finite element predictions of cartilage contact stresses in the hip. *J Biomech*,43(7):1351–1357.
20. Damsgaard M, Rasmussen J, Christensen S. T(2006)Analysis of musculoskeletal systems in the AnyBody Modeling System[J]. *Simulation Modelling Practice and Theory*,14(8): 1100–1111.
21. Niknafs N, Murphy RJ, Armiger RS, Lepistö J, Armand M. Biomechanical factors in planning of periacetabular osteotomy. *Front Bioeng Biotechnol.* 2013;10:1:20.
22. Zou Z, Chávez-Arreola A, Mandal P, Board TN, Alonso-Rasgado. T(2013)Optimization of the position of the acetabulum in a ganz periacetabular osteotomy by finite element analysis. *J Orthop Res*,31(3):472–479.
23. Kharb A, Saini V, Jain Y. K(2011)A review of gait cycle and its parameters[J].*IJCEM International Journal of Computational Engineering & Management*,13:78–83.
24. Phillips AT, Pankaj P, Howie CR, Usmani AS, Simpson AH. Finite element modelling of the pelvis: inclusion of muscular and ligamentous boundary conditions. *Med Eng Phys.* 2007;29(7):739–48.
25. Caligaris M, Ateshian GA. Effects of sustained interstitial fluid pressurization under migrating contact area, and boundary lubrication by synovial fluid, on cartilage friction. *Osteoarthritis Cartilage.* 2008;16(10):1220–7.
26. Bergmann G, Deuretzbacher G, Heller M, Graichen F, Rohlmann A, Strauss J, Duda GN. Hip contact forces and gait patterns from routine activities. *J Biomech.* 2001;34(7):859–71.

27. Krebs DE, Robbins CE, Lavine L, Mann. RW(1998)Hip biomechanics during gait. *J Orthop Sports Phys Ther*,28(1):51–59.
28. Luo C, Wu XD, Wan Y, Liao J, Cheng Q, Tian M, Bai Z, Huang W(2020)Femoral Stress Changes after Total Hip Arthroplasty with the Ribbed Prosthesis: A Finite Element Analysis. *Biomed Res Int*,2020:6783936.
29. Shankar S, Nithyaprakash R, Santhosh BR, Uddin MS, Pramanik. A(2020)Finite element submodeling technique to analyze the contact pressure and wear of hard bearing couples in hip prosthesis. *Comput Methods Biomech Biomed Engin*,23(8):422–431.
30. Kitamura K, Fujii M, Utsunomiya T, Iwamoto M, Ikemura S, Hamai S, Motomura G, Todo M, Nakashima. Y(2020)Effect of sagittal pelvic tilt on joint stress distribution in hip dysplasia: A finite element analysis. *Clin Biomech (Bristol, Avon)*,74:34–41.
31. Abdullah AH, Todo M, Nakashima. Y(2017)Prediction of damage formation in hip arthroplasties by finite element analysis using computed tomography images. *Med Eng Phys*,44:8–15.doi:10.1016/j.medengphy.2017.03.006.
32. Genda E, Iwasaki N, Li G, MacWilliams BA, Barrance PJ. Chao EY(2001)Normal hip joint contact pressure distribution in single-leg standing—effect of gender and anatomic parameters. *J Biomech*,34(7):895–905.
33. Mavcic B, Pompe B, Antolic V, Daniel M, Iglic A, Kralj-Iglic. V(2002)Mathematical estimation of stress distribution in normal and dysplastic human hips. *J Orthop Res*,20(5):1025–1030.doi:10.1016/S0736-0266(02)00014-1.
34. Brown TD, Shaw. DT(1983)In vitro contact stress distributions in the natural human hip. *J Biomech*,16(6):373–384.
35. Wang G, Huang W, Song Q, Liang. J(2017)Three-dimensional finite analysis of acetabular contact pressure and contact area during normal walking. *Asian J Surg*,40(6):463–469.
36. Anderson AE, Ellis BJ, Maas SA, Peters CL, Weiss. JA(2008)Validation of finite element predictions of cartilage contact pressure in the human hip joint. *J Biomech Eng*,130(5):051008.
37. Harris MD, Anderson AE, Henak CR, Ellis BJ, Peters CL. Weiss JA(2012)Finite element prediction of cartilage contact stresses in normal human hips. *J Orthop Res*,30(7):1133–1139.
38. Wu H-H, Wang D, Ma A-B. Dong-Yun Gu(2016)Hip joint geometry effects on cartilage contact stresses during a gait cycle. *Conf Proc IEEE Eng Med Biol Soc*,2016:6038–6041.
39. Li J. Development and validation of a finite-element musculoskeletal model incorporating a deformable contact model of the hip joint during gait. *J Mech Behav Biomed Mater*. 2021;113:104136.
40. Genda E, Konishi N, Hasegawa Y, Miura. T(1995)A computer simulation study of normal and abnormal hip joint contact pressure. *Arch Orthop Trauma Surg*,114(4):202–206.
41. Armiger RS, Armand M, Tallroth K, Lepistö J. Mears SC(2009)Three-dimensional mechanical evaluation of joint contact pressure in 12 periacetabular osteotomy patients with 10-year follow-up. *Acta Orthop*,80(2):155–161.
42. Mukherjee K, Gupta S. The effects of musculoskeletal loading regimes on numerical evaluations of acetabular component. *Proc Inst Mech Eng H*. 2016;230(10):918–29.
43. Fernandez J, Sartori M, Lloyd D, Munro J, Shim. V(2014)Bone remodelling in the natural acetabulum is influenced by muscle force-induced bone stress. *Int J Numer Method Biomed Eng*,30(1):28–41.
44. Hua X, Li J, Jin Z, Fisher. J(2016)The contact mechanics and occurrence of edge loading in modular metal-on-polyethylene total hip replacement during daily activities. *Med Eng Phys*,38(6):518–525.

45. Dikko Kaze A, Maas S, Arnoux PJ, Wolf C, Pape D(2017)A finite element model of the lower limb during stance phase of gait cycle including the muscle forces. Biomed Eng Online,16(1):138.doi:10.1186/s12938-017-0428-6.
46. Hu Z, Ren L, Hu D, Gao Y, Wei G, Qian Z, Wang K. Speed-Related Energy Flow and Joint Function Change During Human Walking. Front Bioeng Biotechnol. 2021;31:9:666428.

## Figures

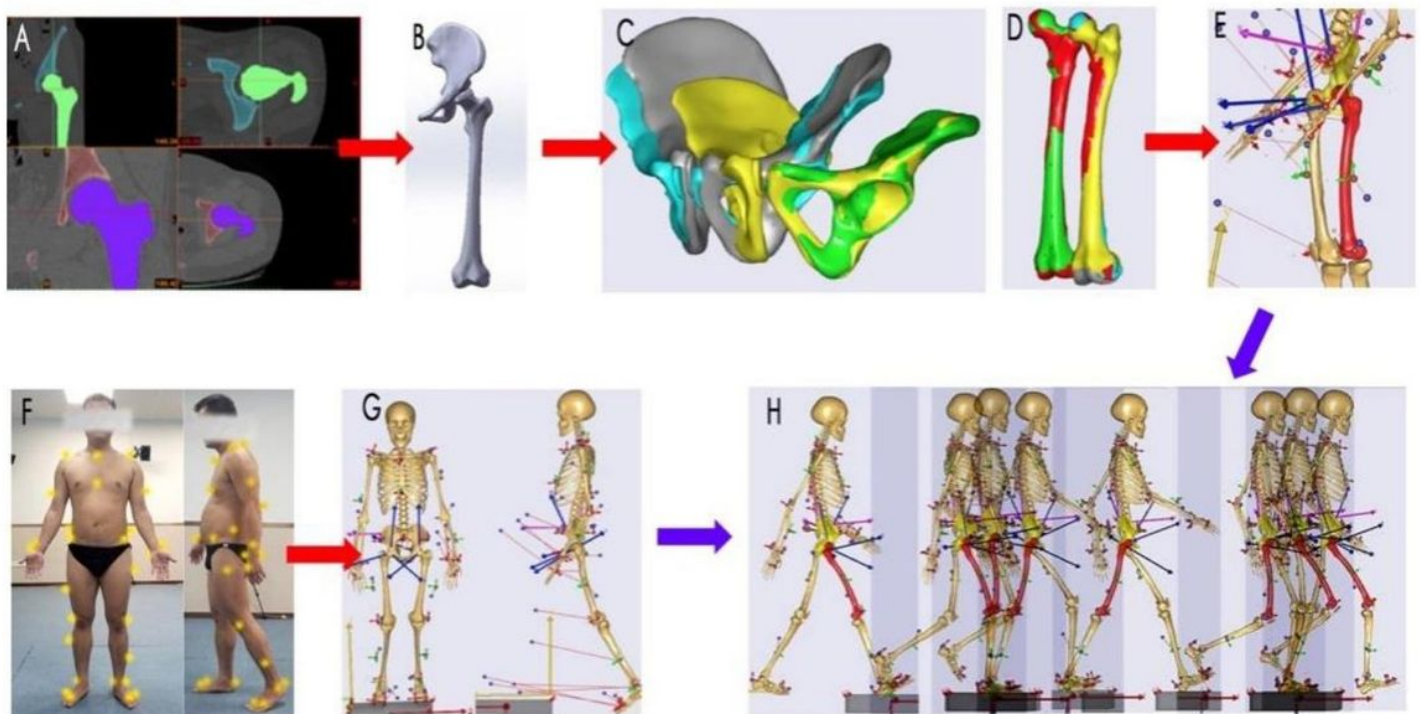


**Figure 1**

The workflow of a subject-specific musculoskeletal dynamic modeling (A & B, geometric reconstruction based on 3D CT data of normal hips; C & D, the scaling of iliac and femur morphology; E, a subject-specific musculoskeletal model after registration with geometric data; F & G, collection and introduction of subject-specific gait data; H, the dynamic hip motion of a subject-specific musculoskeletal model using kinematic analysis)

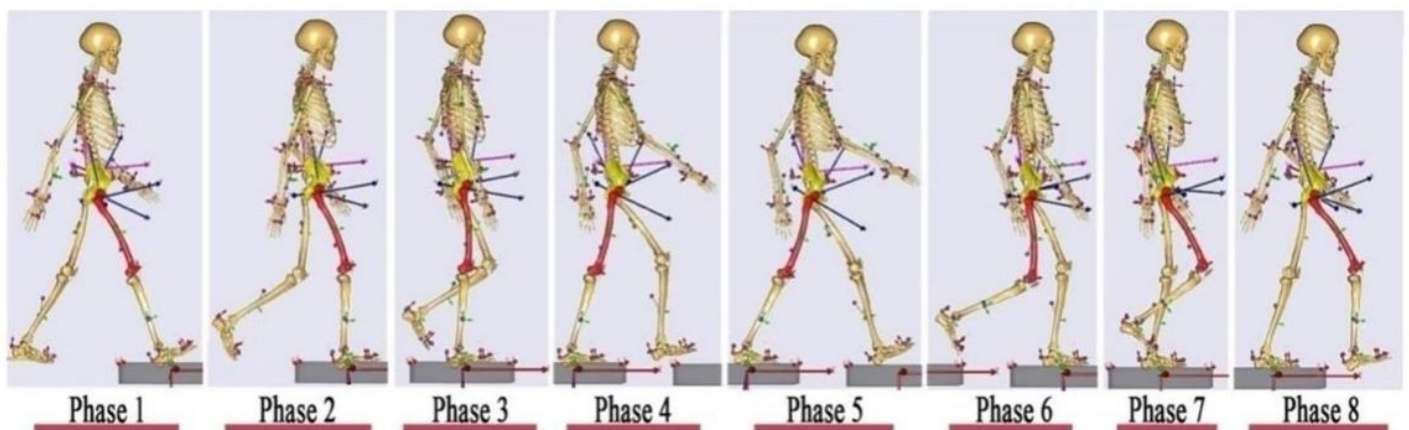


**Figure 2**

Schematic diagram of the 8 phases in a gait cycle using a subject-specific kinematic model (a gait cycle: phase 1, the initial contact phase; phase 2, the loading response phase; phase 3, the mid-stance phase; phase 4, the terminal stance phase; phase 5, the pre-swing phase; phase 6, the initial swing phase; phase 7, the mid-swing phase; and phase 8, the terminal swing phase)

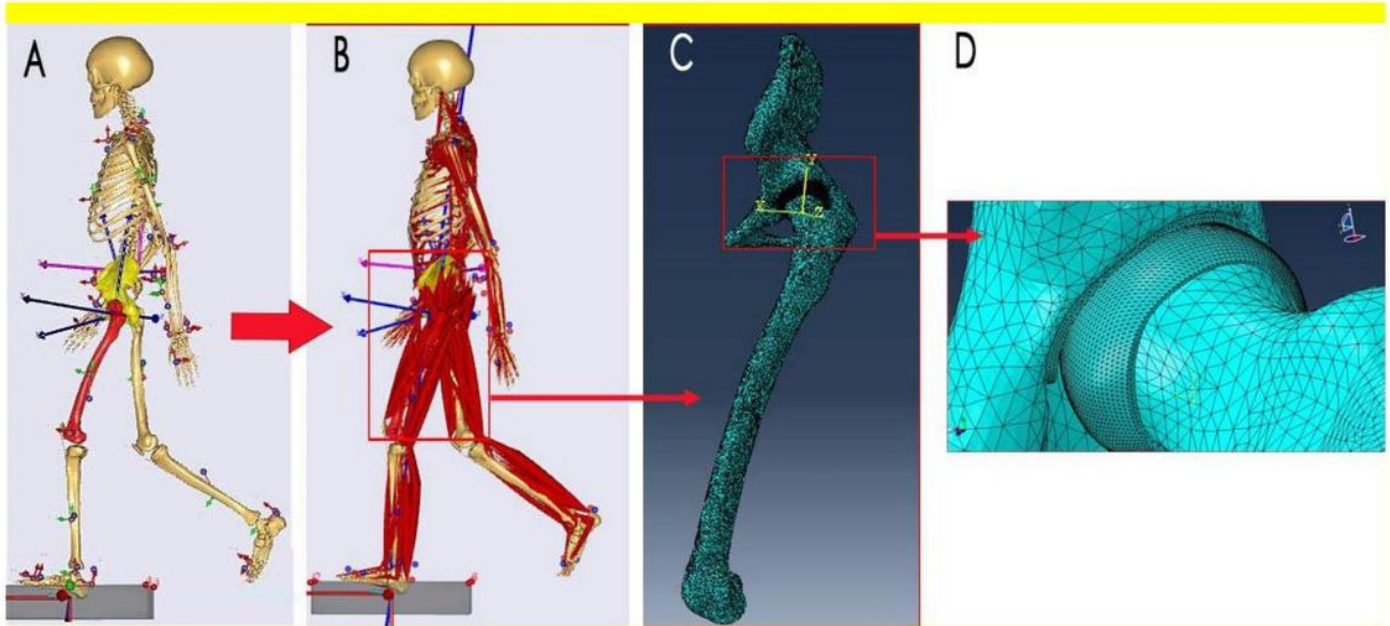


**Figure 3**

The musculoskeletal model versus the FE model in the phase 2 of a gait cycle (A & B, a subject-specific gait simulation using the kinematic analysis and inverse dynamic analysis; C, the hip joint in an FE model; D, the contact stress distribution in the femoral head and the acetabulum of an FE model)

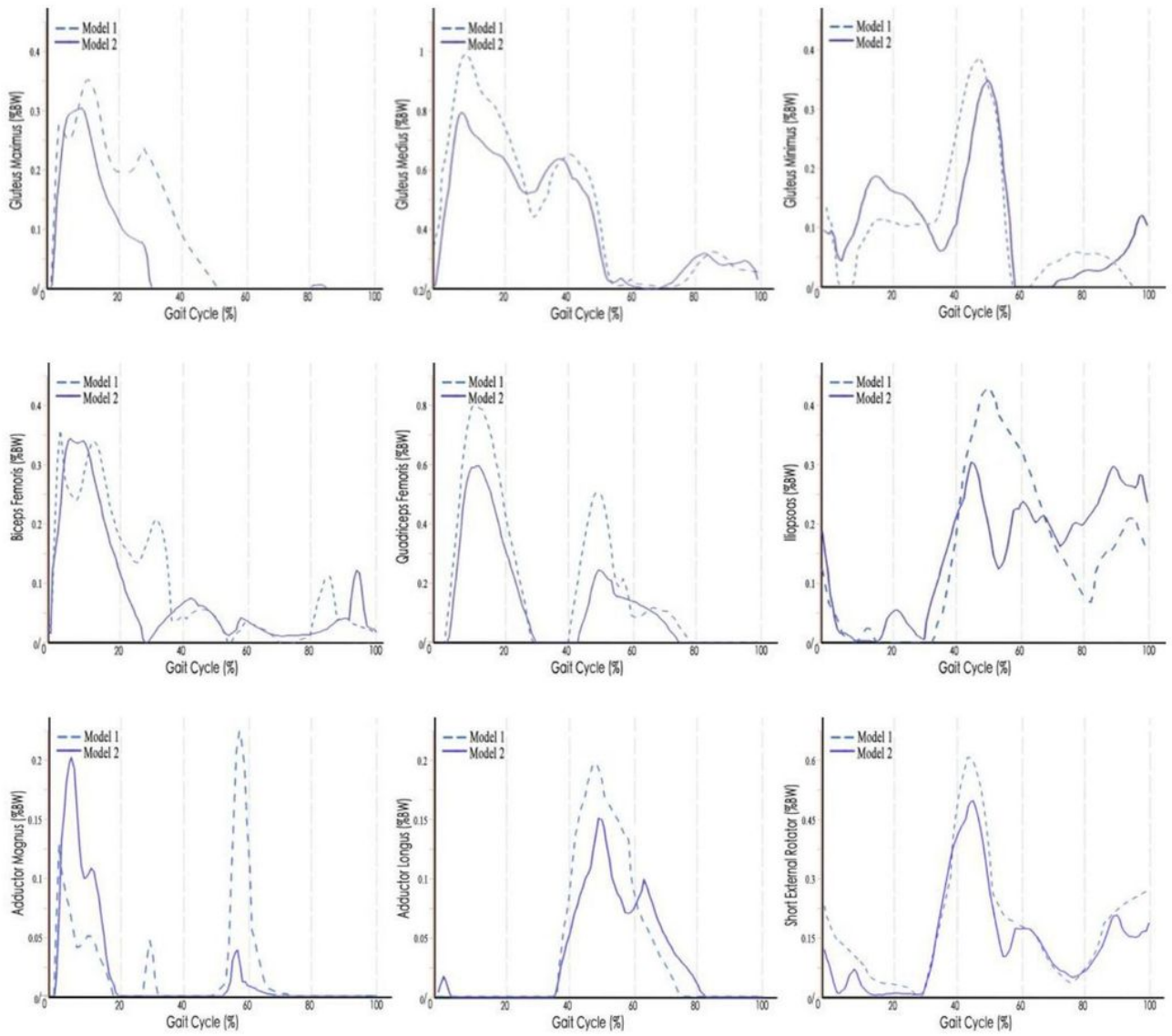


**Figure 4**

Muscle force patterns during a normal gait cycle using subject-specific musculoskeletal models

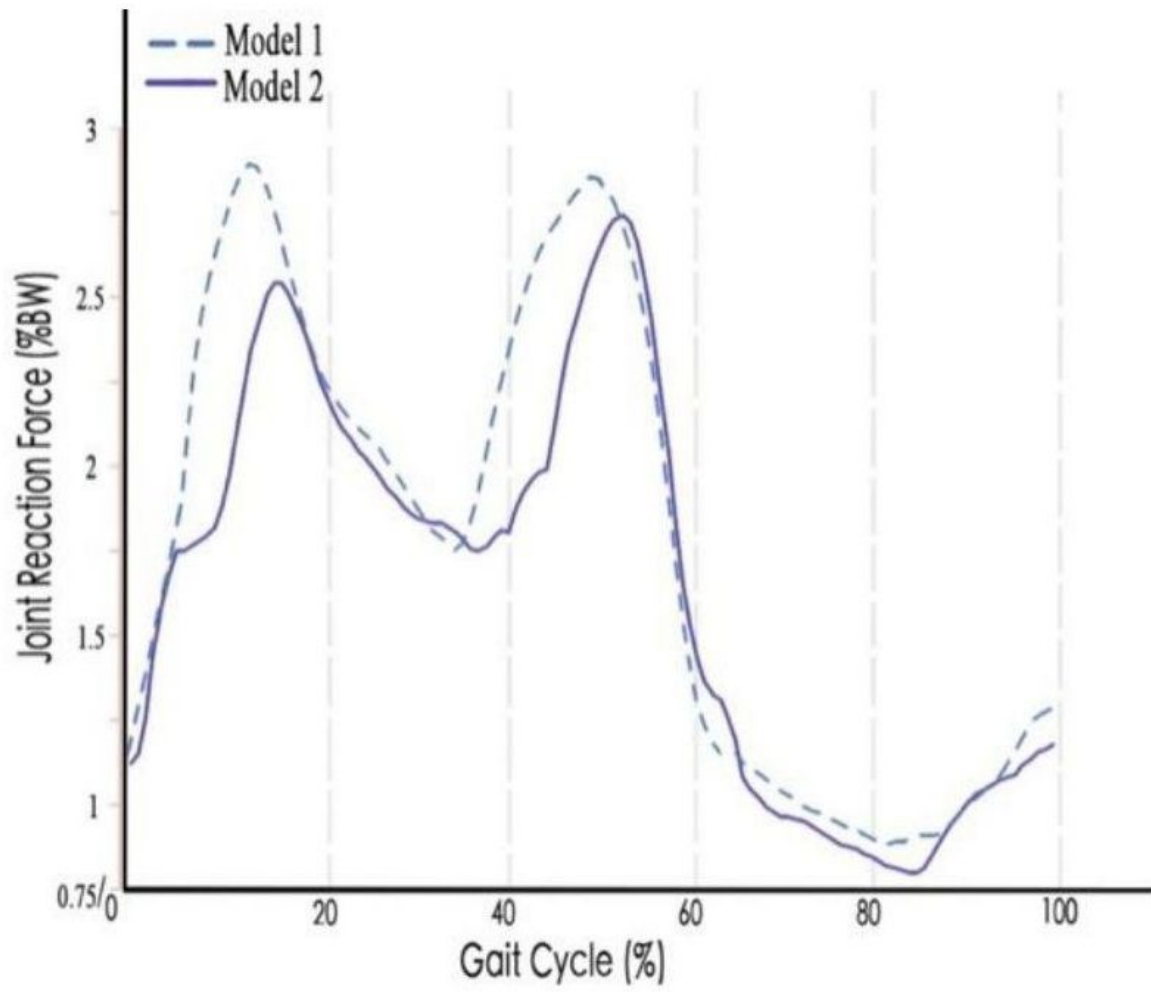


**Figure 5**

Hip joint reaction forces for subject-specific musculoskeletal models during gait cycle.

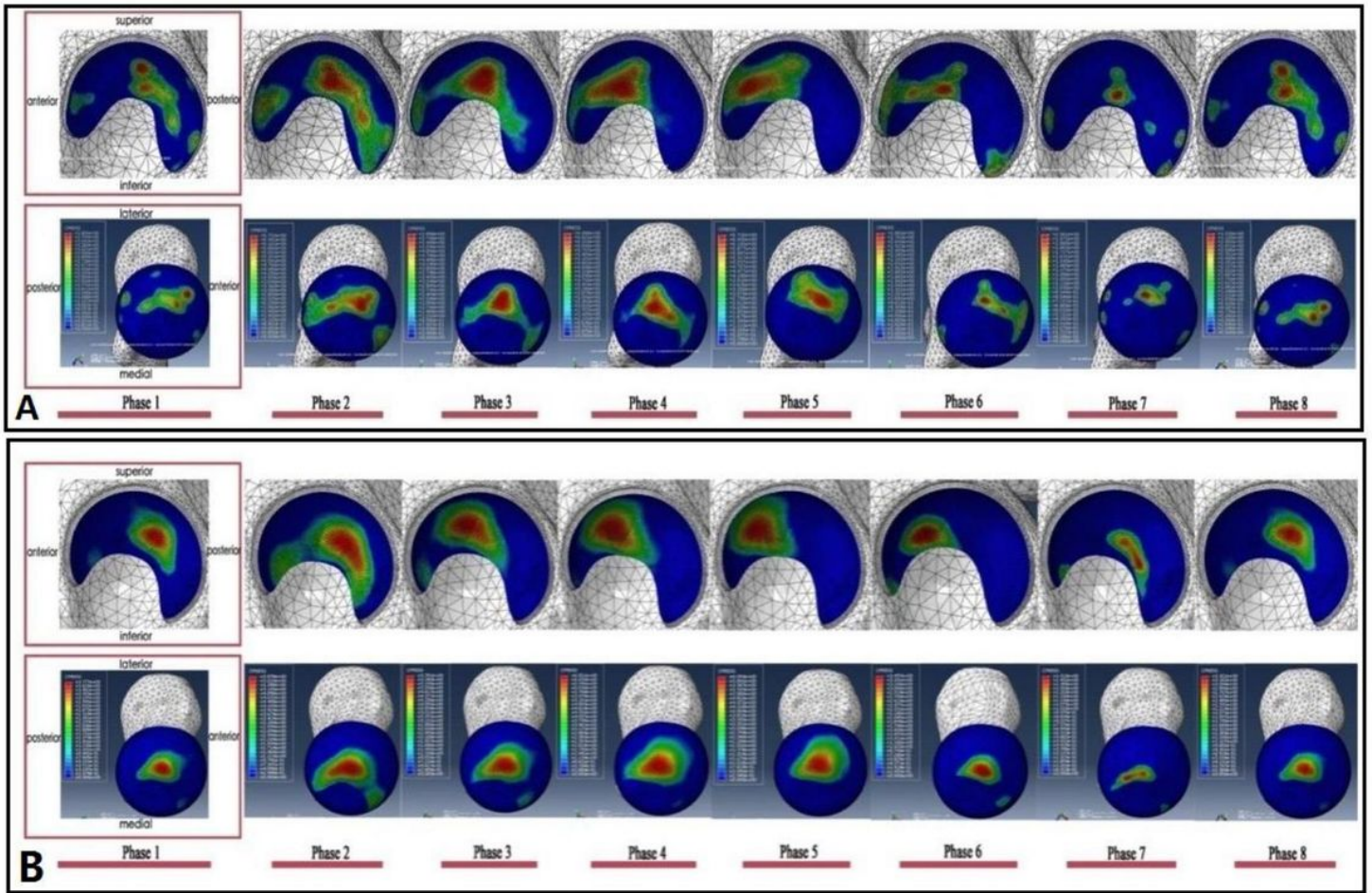


**Figure 6**

The nephograms of the contact pressure (CPRESS) on the acetabulum and femoral head cartilage surface during each phase of a gait cycle. A: Model 1, B: Model 2.